International Journal of Mining Engineering and Mineral Processing 2018, 7(1): 1-13
DOI: 10.5923/j.mining.20180701.01

Correlations between Point Load Strength Index and Physical Properties of Hydrothermally Altered Rocks

Masanori Kohno[1,*], Hiroyuki Maeda[2]

[1]Faculty of Engineering, Tottori University, Tottori, Japan
[2]Sapporo Technology Professional Training College, Sapporo, Japan

Abstract The purpose of this study was to clarify the correlation between point load strength index and several physical properties in hydrothermally altered rocks, which are typical of the soft rocks found in northeastern Hokkaido, Japan, using axial and irregular lump point load strength test specimens. The numbers of specimens tested were 3,828 rock specimens for the point load strength test. These came primarily from the earth's surface in ancient hydrothermal fields. The rock specimens underwent point load strength test using a laboratory testing machine with specimens in dry and saturated conditions. This study clarified the decrease in strength that can be assessed by measuring the elastic wave velocity. In addition, the results suggest that future landslide and collapse potential within a hydrothermal area can be assessed based on the hydrothermal alteration type, and point load strength index change ratio.

Keywords Point load strength index, Physical property, Hydrothermally altered rock

1. Introduction

The strength of fresh rocks and altered rocks, as well as hydrothermally altered or weathered rocks, is generally evaluated based on uniaxial compressive strength (UCS). However, rock core pieces for UCS tests cannot always be obtained from outcrops of faulted, jointed or cracked rock masses. In these cases, the point load strength (PLS) test is a convenient and an effective alternative to the UCS test, because it can be done promptly using on-site testing equipment with various shaped small rock specimens taken from outcrops or floats. Many researchers have already studied the relationship between the PLS and UCS of soft rocks. For example, UCS = 13 PLS [1], UCS = 13.4 PLS [2], UCS = 16.4 PLS [3]. Some researchers have obtained a correlation between the PLS index and physical properties of rocks [4-8]. On the other hand, many researchers have studied the physical properties of altered rocks [9-18]. However, there are very few reports about the correlation between the PLS index and physical properties of soft rocks. Furthermore, when we examine the relationship for real between PLS and physical properties of rocks that we sampled, we will notice that they are not necessary subject to the relationships mentioned in existing studies. Especially, with regard to hydrothermally altered rocks, we will need to do the research about the relationship between PLS and physical properties of such rocks, because there is still little data available for it. One of the reasons why the correlation between the PLS index and physical properties of soft rocks have not been established is the difficulty in collecting and testing samples because of the influence of swelling clay minerals and other factors; the other reason is that the hard rocks with relatively major occurrence are found particularly in North America, Europe, and other places. However, it is important to determine the correlation between the PLS index and physical properties of soft rocks widely found in Japan, the Pacific Rim region, and other places.

The purpose of this study was to determine the correlation between the PLS index and physical properties (density, water absorption, effective porosity, and elastic wave velocity) of hydrothermally altered rocks using axial and irregular lump PLS test specimens; these altered rocks are typically soft rocks found in northeastern Hokkaido, Japan. Furthermore, we clarified the relationship between the PLS index and physical properties of hydrothermally altered rocks based on the PLS index change ratio. In addition, we have obtained a significant result by examining the relationship between the PLS index change ratio and hydrothermally altered rocks.

2. Rock Samples

A majority of the samples were collected from the Okushunbetsu area in Teshikaga Town, Japan. Figures 1 and

* Corresponding author:
kohnom@tottori-u.ac.jp (Masanori Kohno)
Published online at http://journal.sapub.org/mining

2 show the geological map and distribution of hydrothermal alteration zones in the Okushunbetsu area. The geology of the sampling sites consisted primarily of the Upper Miocene Oteshikaushinai, Hanakushibe, and Shikerepe Formations, and the Upper Pliocene Shikerepeyama Lava in the Okushunbetsu area of Teshikaga Town, northeastern Hokkaido, Japan. The geology and the distribution of hydrothermal alteration zones in this district were described mainly by Maeda et al. [19].

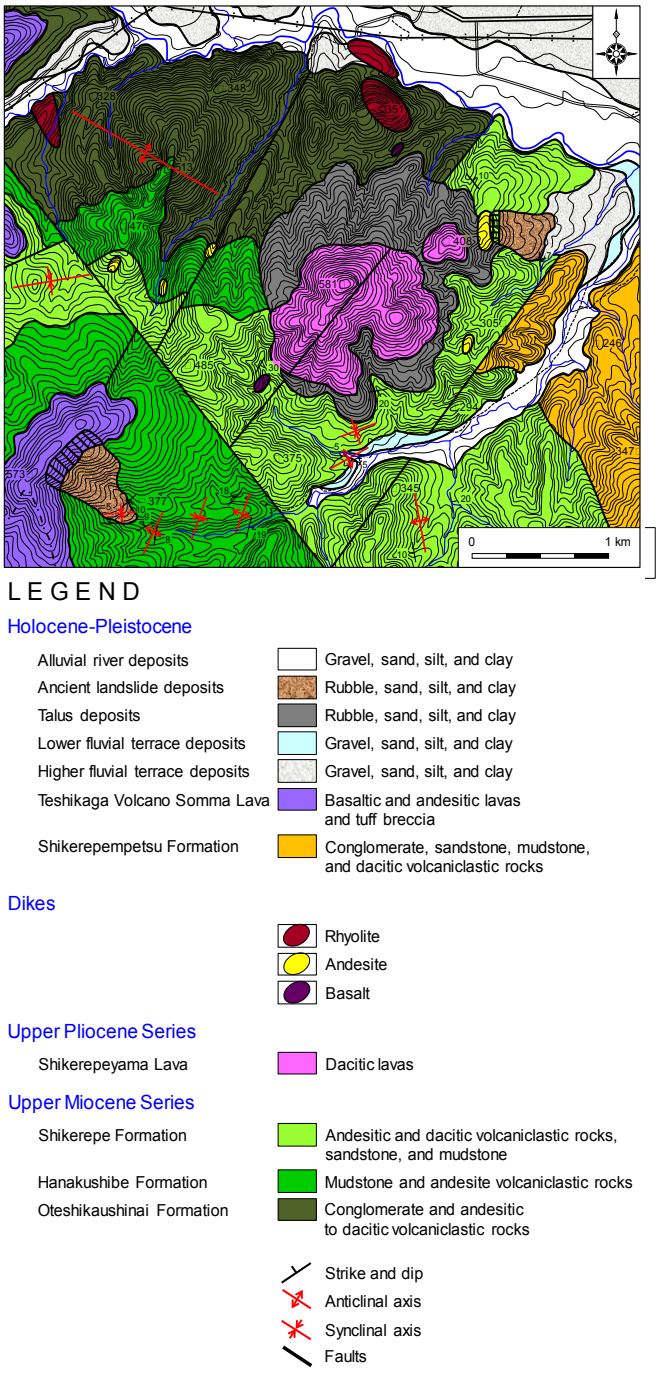

Figure 1. Geological map in the Okushunbetsu area, Teshikaga Town (modified from Maeda et al. [19])

The rock samples, which were collected primarily from the earth's surface in ancient hydrothermal fields, were hydrothermally altered volcaniclastic rocks, including fine tuff, medium tuff, pumice tuff, lapilli tuff, welded tuff, dacite, tuffaceous mudstone, tuffaceous sandstone, and tuffaceous conglomerate. The modes of occurrence of these hydrothermally altered rocks were examined in the field, and the hydrothermal alteration minerals in the rocks were identified primarily by X-ray powder diffraction (XRD) test (Figure 3 and Table 1). Clay minerals in the hydrothermally altered rocks were identified from XRD patterns of untreated and ethylene glycol-treated oriented samples. The XRD test was performed using a Rigaku RINT Ultima+ diffractometer (30 kV, 20 mA) equipped with a copper tube, a 0.30-mm receiving slit, and 1° divergence and scattering slits. Hydrothermal alteration can be zonated according to the occurrence of characteristic minerals [20]. The hydrothermal alteration zone can be divided into 15 more specific zones (Figure 4), based on the mineral assemblages of hydrothermally altered rocks. The hydrothermal alteration zone is composed of alunite-quartz, dickite, halloysite, propylitic, K-feldspar, illite, interstratified illite/smectite mineral, interstratified chlorite/smectite mineral, smectite, laumontite, analcite, heulandite, mordenite, clinoptilolite, and stilbite zones (Figures 3 and 4, and Table 1). Classification of hydrothermal alteration zones based on temperature and activity ratio of aqueous cation species in the hydrothermal solution have been described by Utada [20].

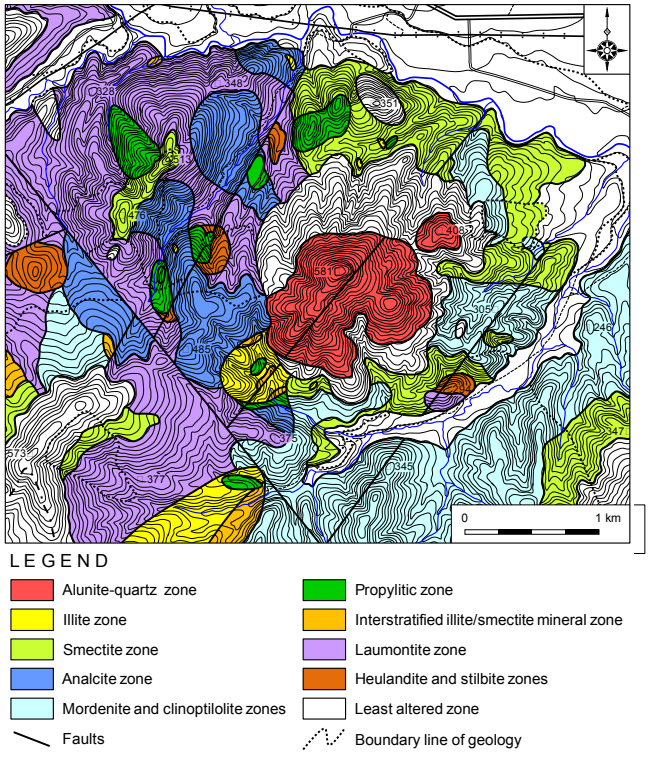

Figure 2. Distribution of hydrothermal alteration zones in the Okushunbetsu area, Teshikaga Town (modified from Maeda et al. [19])

3. Methods and Equipment

3.1. Point Load Strength Test

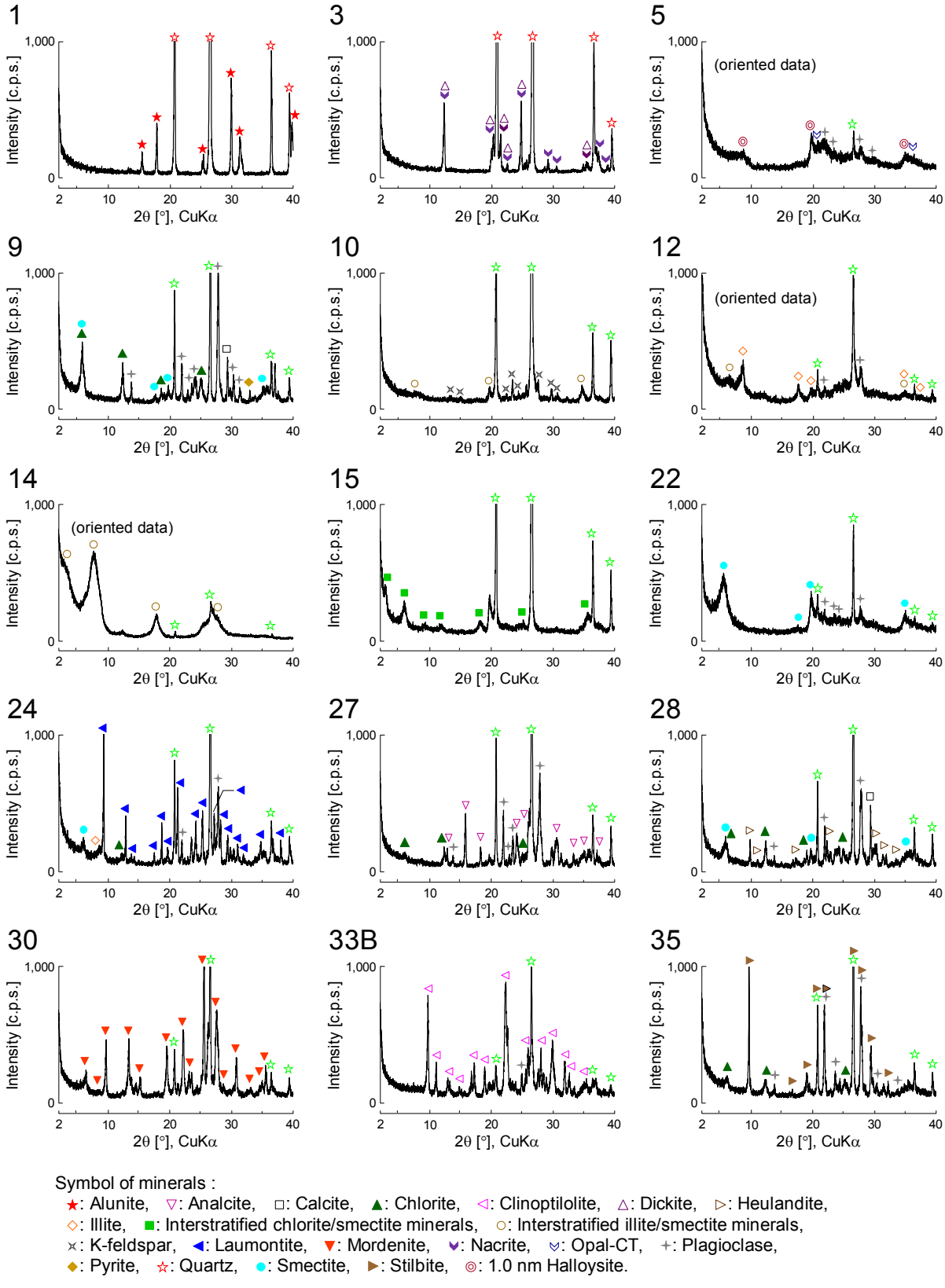

Figure 3. X-ray powder diffraction patterns of hydrothermal altered rocks. Numbers correspond to "Rock code" in Tables 1 and 2

Table 1. Rock type, semi-quantitative mineral composition, and hydrothermal alteration zone of hydrothermally altered rocks

Rock code	Rock type	Semi-quantitative mineral composition	Hydrothermal alteration zone
1	Dacite	Qz (+), Alu (+)	Alunite-quartz zone
2	Dacite	Qz (+), Alu (+), Kao (-), Carbonates (-)	Alunite-quartz zone
3	Fine tuff	Qz (+), Nac (-), Dck (-)	Dickite zone
4	Fine tuff	Qz (+), Nac (-), Dck (-)	Dickite zone
5	Pumice tuff	Qz (-), Opl-CT (-), Pl (-), 1.0 nm Ha (-)	Halloysite zone
6	Tuffaceous conglomerate	Qz (-), Opl-CT (-), Pl (-), 1.0 nm Ha (-)	Halloysite zone
7	Fine tuff	Qz (-), Pl (-), Chl (+), Sme and/or Chl/Sme (-)	Propylitic zone
8	Medium tuff	Qz (+), Pl (-), Ilt (-), Chl (-)	Propylitic zone
9	Lapilli tuff	Qz (+), Pl (-), Chl (-), Sme (-), Py (-)	Propylitic zone
10	Fine tuff	Qz (+), Kfs (-), Chl (?), Ilt/Sme (-), Sme (?)	K-feldspar zone
11	Fine tuff	Qz (+), Kfs (-), Chl (?), Ilt/Sme (-), Sme (?)	K-feldspar zone
12	Tuffaceous sandstone	Qz (+), Pl (-), Ilt (-), Sme (-), Ilt/Sme (-)	Illite zone
13	Tuffaceous sandstone	Qz (+), Pl (-), Ilt (-), Sme (-), Ilt/Sme (-), Hul-Cpt (-)	Illite zone
14	Tuffaceous mudstone	Qz (+), Pl (-), Ilt (-), Chl (-), Sme (-), Ilt/Sme (-)	Ilt/Sme zone
15	Fine tuff	Qz (+), Chl/Sme (-)	Chl/Sme zone
16	Fine tuff	Qz (+), Fsp (-), Sme (-)	Smectite zone
17	Fine tuff	Qz (-), Opl-A (-), Fsp (-), Sme (-), Mor or Cpt (-)	Smectite zone
18	Fine tuff	Qz (-), Opl-A (-), Pl (-), Sme (-)	Smectite zone
19	Fine tuff	Qz (+), Pl (-), Sme (-)	Smectite zone
20	Pumice tuff	Qz (-), Opl-A (-), Fsp (-), Sme (+)	Smectite zone
21	Pumice tuff	Qz (-), Opl-A (-), Fsp (-), Sme (+)	Smectite zone
22	Pumice tuff	Qz (-), Opl-A (-), Fsp (-), Sme (+)	Smectite zone
23	Fine tuff	Qz (+), Pl (+), Sme (-), Lmt (-)	Laumontite zone
24	Lapilli tuff	Qz (+), Pl (-), Ilt (-), Chl (-), Sme (-), Lmt (+)	Laumontite zone
25	Tuffaceous conglomerate	Qz (-), Pl (+), Chl (-), Lmt (-), Cal (+), Py (-)	Laumontite zone
26	Tuffaceous conglomerate	Qz (+), Pl (+), Chl (-), Sme (-), Lmt (-), Cal (-)	Laumontite zone
27	Fine tuff	Qz (+), Pl (-), Ilt (-), Chl (-), Anl (+)	Analcite zone
28	Lapilli tuff	Qz (+), Pl (-), Chl (-), Sme (-), Hul (-), Cal (-)	Heulandite zone
29A	Fine tuff	Qz (-), Fsp (-), Sme (-), Mor (+), Cpt (-)	Mordenite zone
29B	Fine tuff	Qz (-), Fsp (-), Sme (-), Mor (+), Cpt (-)	Mordenite zone
29C	Fine tuff	Qz (-), Fsp (-), Sme (-), Mor (+), Py (-)	Mordenite zone
29D	Fine tuff	Qz (-), Fsp (-), Sme (-), Mor (+)	Mordenite zone
29E	Fine tuff	Qz (-), Fsp (-), Sme (-), Mor (+)	Mordenite zone
29F	Fine tuff	Qz (+), Fsp (-), Sme (-), Mor (+)	Mordenite zone
30	Fine tuff	Qz (-), Mor (+)	Mordenite zone
31	Pumice tuff	Qz (+), Fsp (-), Sme (-), Mor (+), Lmt (-)	Mordenite zone
32	Pumice tuff	Qz (-), Fsp (-), Sme (-), Mor (+), Lmt (-)	Mordenite zone
33A	Fine tuff	Qz (-), Fsp (-), Sme (-), Cpt (+)	Clinoptilolite zone
33B	Fine tuff	Qz (+), Fsp (-), Sme (-), Cpt (-)	Clinoptilolite zone
34	Fine tuff	Qz (+), Pl (-), Sme (-), Cpt (-)	Clinoptilolite zone
35	Tuffaceous sandstone	Qz (+), Pl (-), Chl (-), Sme and/or Chl/Sme (-), Stb (+)	Stilbite zone
36	Welded tuff	Qz (-), Opl-A (-), Opl-CT (-), Pl (+)	Least altered zone
37	Welded tuff	αCrs (+), βCrs (-), Pl (+), Kfs (-)	Least altered zone
38	Welded tuff	Opl-A (-), Opl-CT (-), Pl (-)	Least altered zone

Alu: Alunite, Anl: Analcite, Cal: Calcite, Chl: Chlorite, Chl/Sme: Interstratified chlorite/smectite minerals, Chl/Sme zone: Interstratified chlorite/smectite mineral zone, Cpt: Clinoptilolite, Crs: Cristobalite, Dck: Dickite, Fsp: Feldspar, Ha: Halloysite, Hul: Heulandite, Hul-Cpt: Heulandite-clinoptilolite series minerals, Ilt: Illite, Ilt/Smc: Interstratified illite/ smectite minerals, Ilt/Sme zone: Interstratified illite/smectite mineral zone, Kao: Kaolin minerals, Kfs: K-feldspar, Lmt: Laumontite, Mor: Mordenite, Nac: Nacrite, Opl-A: Opal-A, Opl-CT: Opal-CT, Pl: Plagioclase, Py: Pyrite, Qz: Quartz, Sme: Smectite, Stb: Stilbite, + : Large amounts, - : Small amounts.

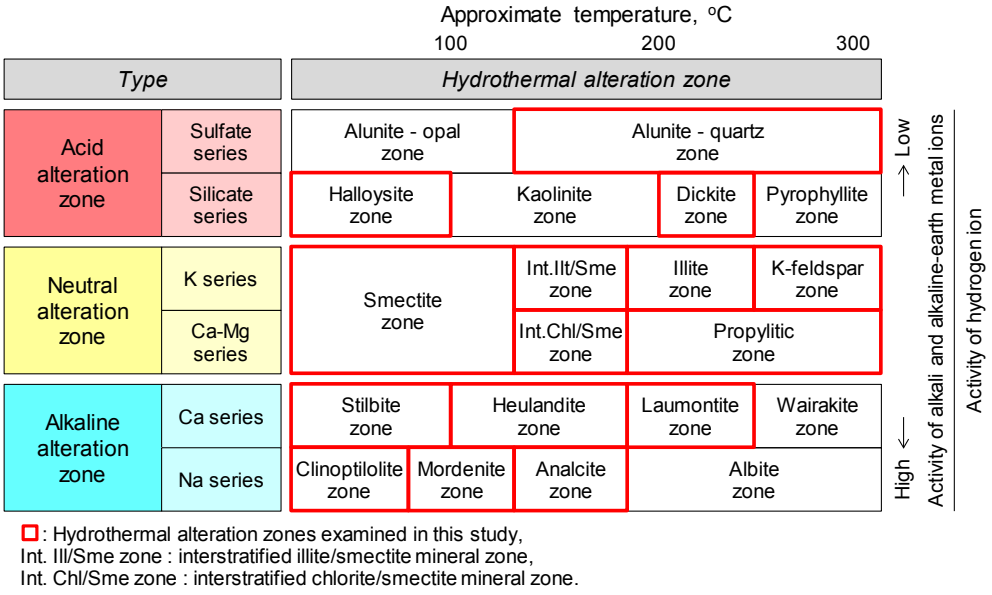

Figure 4. Classification of hydrothermal alteration zones based on temperature and activity ratio of aqueous cation species in the hydrothermal solution (modified from Utada [20])

The PLS test was conducted in accordance with the ISRM Commission [21]. In the PLS tests, the specimens were loaded to failure by application of a concentrated load through a pair of spherically truncated, conical platens. The testing machine consisted of conical loading platens, loading frame, dial gauge, manual control handle, load cell, and load measuring system. The loading speed was set so that each specimen failed within 10–60 s. This was achieved using a manual control handle by loading each specimen continuously at a constant (as much as possible) loading speed up to approximately 100 N/s of load increase. The size-corrected PLS index of a rock specimen was defined as the value of PLS that would have been measured by a diametral PLS test with a diameter D = 50 mm (D_e^2 = 2,500 mm^2 where D_e is the equivalent core diameter). The PLS index can be represented by the formula:

$$I_{s(50)} = F\frac{P}{D_e^2} \tag{1}$$

where $I_{s(50)}$ is the PLS index (corrected PLS of specimen), F is the size correction factor, P is the peak load (failure load), and D_e is the equivalent core diameter. D_e is the diameter of a circle with an area equal to the minimum area of the cross sections containing the two loading points, and can be represented by the formula:

$$D_e^2 = \frac{4WD'}{\pi} \tag{2}$$

where D_e is the equivalent core diameter, W is the specimen width, and D' is the distance between the two loading platens at the time of failure. The ISRM Commission [21] stipulated that if significant penetration of the conical platens occurs during the test, such as when testing soft rocks, the value of D' should be the final value of the distance between the two loading platens. Therefore, in this study, the PLS was calculated using the distance between the two loading platens at the time of failure:

$$D' = D - \alpha \tag{3}$$

where D' is the distance between the two loading platens at the time of failure, D is the distance between the two loading platens, and α is the penetration distance of the conical platens. The distance between the two loading platens and the penetration distance of the conical platens were measured using slide calipers and a dial gauge (analog type), respectively. F can be represented by the formula:

$$F = \left(\frac{D_e}{50}\right)^{0.45} \tag{4}$$

where F is the size correction factor and D_e is the equivalent core diameter. The PLS tests in this study were performed using a laboratory testing machine with specimens in dry and wet conditions.

3.2. Physical Tests

The physical test was conducted in accordance with the ISRM Commission [22]. The density (dry: ρ_d and saturated: ρ_{sat}), water absorption Q, and effective porosity n are given by:

$$\rho_d = \frac{m_s}{V} \tag{5}$$

$$\rho_{sat} = \rho_d + n\rho_w \tag{6}$$

$$Q = \frac{m_{sat} - m_s}{m_s} \times 100\ (\%) \tag{7}$$

$$n = \frac{V_v}{V} = \frac{m_{sat} - m_s}{m_{sat} - m_{sub}} \times 100\ (\%) \tag{8}$$

where m_s is the dry mass, m_{sat} is the saturated mass, m_{sub} is the submerged mass, ρ_w is density of water, V is the apparent volume by buoyancy method, and V_v is the pore volume. The elastic wave velocity test was performed using a Fuji Bussan Co., Ltd. PUNDIT (minimum measurement interval: ±0.1 μs) testing machine. The elastic wave velocity V_p is given by:

$$V_p = \frac{h}{t} \tag{9}$$

where h is height of the specimen and t is the travel time.

3.3. Test Specimen Preparation

In this study, axial and irregular lump specimens were used for the PLS tests (Figure 5). The rock specimens used for the axial PLS test in this study were drilled to a diameter of 50 mm and cut to a length of 20 mm using a diamond cutter. This shape was easy to produce, having the advantage of using drilled cores, and it satisfied the conditional expression of $0.3W < D < W$ [21] (Figure 5A). The rock specimens used for the irregular lump PLS test in this study had an average diameter of approximately 50 mm, and the distance between the two loading platens was approximately 30 mm. The irregular lump PLS test specimen size satisfied the conditional expression of $0.3W < D < W$ and $0.5D < L$ [21] (Figure 5B).

A total of 38 different rock types were sampled, and the total number of rock specimens tested was 3,828 for the PLS tests (Table 2). The number of specimens in Table 2 did not include invalid test specimens.

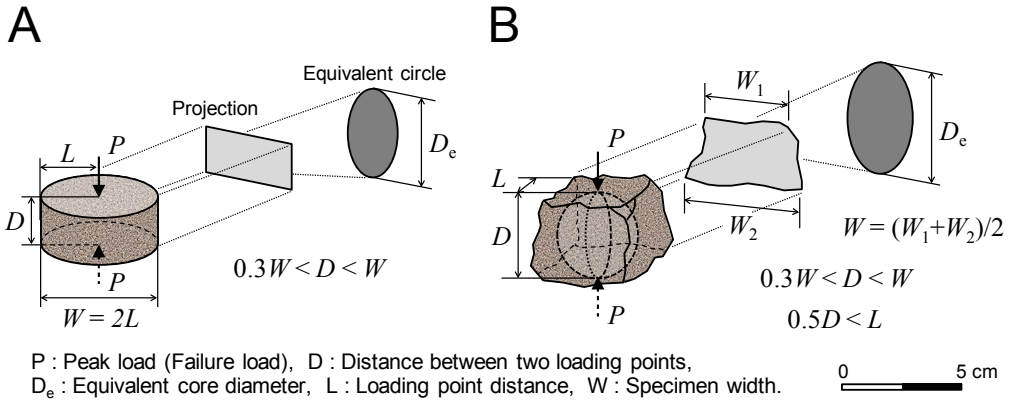

Figure 5. Shape of rock specimens, load configuration, and conditional expression for axial point load strength test (A) and irregular lump point load strength test (B)

Table 2. Numbers of specimens and results of the point load strength test

Rock code	Dry condition				Saturated condition				*PCR* [%]
	N	$I_{s(50)}$ [MPa]	$I_{s(50)}$ range [MPa]	C_v [%]	*N*	$I_{s(50)}$ [MPa]	$I_{s(50)}$ range [MPa]	C_v [%]	
1	37	1.15	0.62-1.82	27.9	40	0.97	0.62-1.58	28.8	15.0
2	45	3.06	1.18-5.25	33.4	40	2.21	1.25-3.78	25.7	27.5
3	16	0.36	0.24-0.53	24.7	18	0.13	0.06-0.29	54.2	64.6
4	17	0.17	0.10-0.26	24.0	20	0.07	0.02-0.17	55.7	56.9
5	14	0.28	0.13-0.48	42.8	5	0.12	0.06-0.31	74.9	57.1
6	13	0.40	0.28-0.69	32.6	7	0.05	0.03-0.10	57.0	86.8
7	42	1.45	0.75-2.13	22.1	45	0.57	0.36-0.83	21.0	60.5
8	28	1.25	0.47-2.96	44.8	26	0.87	0.31-1.40	33.2	30.2
9	70	2.38	1.15-3.69	26.0	54	0.84	0.53-1.11	17.8	64.7
10	56	3.52	1.63-6.51	31.3	37	1.60	0.91-3.50	40.9	54.5
11	34	1.52	0.75-2.40	30.9	20	0.93	0.38-1.66	40.0	39.2
12	73	0.51	0.14-0.90	33.1	73	0.14	0.07-0.29	34.8	72.1
13	77	0.52	0.19-0.89	30.7	67	0.14	0.05-0.25	35.7	73.2
14	51	1.58	0.72-2.42	24.0	17	0.16	0.07-0.33	43.9	89.9
15	47	1.26	0.48-1.97	30.2	49	0.05	0.03-0.14	56.8	95.8
16	-	-	-	-	24	0.53	0.27-0.78	30.2	-
17	35	0.77	0.21-1.38	32.5	-	-	-	-	-
18	56	0.25	0.12-0.40	24.1	43	0.12	0.05-0.18	32.8	51.1
19	54	0.71	0.30-1.47	43.5	57	0.12	0.04-0.26	42.0	83.2

Rock code	Dry condition				Saturated condition				*PCR* [%]
	N	$I_{s(50)}$ [MPa]	$I_{s(50)}$ range [MPa]	C_v [%]	*N*	$I_{s(50)}$ [MPa]	$I_{s(50)}$ range [MPa]	C_v [%]	
20	30	0.12	0.07-0.24	32.8	18	0.04	0.01-0.07	53.9	69.5
21	56	0.15	0.08-0.28	25.9	45	0.09	0.03-0.16	45.7	43.4
22	58	0.28	0.14-0.42	28.2	51	0.08	0.02-0.14	39.1	73.0
23	52	0.82	0.38-1.59	35.2	64	0.21	0.08-0.37	32.7	74.1
24	40	0.27	0.07-0.52	48.4	30	0.17	0.09-0.28	30.3	38.6
25	18	2.67	1.59-3.85	23.2	6	1.64	1.20-1.98	15.3	38.8
26	9	2.27	1.42-3.53	29.1	12	0.90	0.50-1.24	26.7	60.4
27	64	0.57	0.21-1.02	38.6	61	0.13	0.03-0.27	44.5	76.4
28	80	1.88	0.85-2.92	31.3	79	0.51	0.23-0.98	37.2	72.9
29A	17	2.39	1.83-3.24	20.5	51	0.70	0.42-0.93	17.2	70.8
29B	25	1.97	1.50-2.52	15.7	35	0.42	0.23-0.68	30.7	78.5
29C	45	2.04	1.33-2.53	13.7	19	0.37	0.27-0.51	19.0	81.9
29D	34	1.28	1.04-1.95	14.9	6	0.37	0.29-0.43	16.3	71.3
29E	39	1.28	0.85-1.53	13.3	11	0.34	0.24-0.55	26.5	73.4
29F	19	1.12	0.88-1.34	14.3	8	0.45	0.24-0.68	44.2	59.6
30	123	1.56	0.32-2.45	22.4	125	0.39	0.16-0.65	30.5	74.8
31	141	1.08	0.49-1.55	20.4	96	0.27	0.08-0.51	43.6	74.5
32	21	0.67	0.39-0.91	21.0	31	0.12	0.08-0.19	25.4	82.3
33A	52	0.84	0.18-1.60	28.7	52	0.24	0.10-0.53	40.9	70.8
33B	30	0.92	0.68-1.22	14.1	67	0.41	0.15-0.57	19.5	55.4
34	40	1.35	0.69-2.55	39.3	36	0.27	0.11-0.59	43.9	79.7
35	110	1.05	0.31-2.12	37.2	86	0.47	0.17-0.85	35.9	54.8
36	51	1.01	0.45-1.50	27.8	50	0.46	0.17-0.84	39.0	54.2
37	68	1.06	0.42-1.36	18.0	66	0.36	0.19-0.45	16.7	66.1
38	49	0.66	0.21-1.31	42.4	45	0.29	0.15-0.54	27.3	55.6

N: number of specimen, $I_{s(50)}$: PLS index, C_v: coefficient of variation, *PCR*: PLS index change ratio.

Table 3. Results of the physical tests

Rock code	Dry density [g/cm^3]	Saturated density [g/cm^3]	Water absorption [%]	Effective porosity [%]	Dry elastic wave velocity [km/s]	Saturated elastic wave velocity [km/s]
1	1.505	1.911	27.07	43.40	2.69	2.47
2	2.177	2.307	5.98	13.14	3.94	3.89
3	1.744	2.070	18.67	33.08	1.93	2.24
4	1.738	2.076	21.17	33.35	1.73	1.54
5	1.358	1.809	25.69	38.02	1.13	1.13
6	1.698	1.788	18.39	28.64	1.08	1.08
7	1.762	2.072	29.44	30.96	2.65	2.46
8	1.891	2.124	12.37	24.11	2.23	2.46
9	1.979	2.218	12.08	24.17	3.33	3.10
10	1.935	2.161	11.72	22.94	3.39	3.24
11	1.858	2.120	14.07	26.22	3.71	3.56
12	1.525	1.811	18.72	30.97	1.51	1.21
13	1.533	1.804	17.69	29.55	1.97	1.55
14	1.813	2.087	17.09	27.66	2.06	1.93
15	1.399	1.827	34.17	45.78	2.02	1.30
16	-	2.039	19.29	36.42	-	1.83
17	1.310	-	34.94	47.74	1.64	-

Rock code	Dry density [g/cm^3]	Saturated density [g/cm^3]	Water absorption [%]	Effective porosity [%]	Dry elastic wave velocity [km/s]	Saturated elastic wave velocity [km/s]
18	0.599	1.334	123.34	74.91	1.03	1.61
19	1.353	1.834	37.75	48.20	1.64	1.28
20	1.079	1.563	44.94	52.23	1.20	1.47
21	1.094	1.552	41.90	48.77	1.47	1.54
22	1.279	1.690	32.13	42.99	1.59	1.76
23	1.550	1.944	25.09	39.31	1.80	1.35
24	1.461	1.829	25.31	38.71	0.98	1.36
25	2.518	2.594	3.02	7.55	3.90	4.28
26	2.309	2.420	4.82	11.12	3.52	3.74
27	1.526	1.947	31.05	42.20	2.15	2.09
28	1.772	2.054	18.84	28.36	2.73	2.23
29A	1.284	1.728	34.84	44.56	1.85	2.33
29B	1.191	1.749	37.53	48.62	1.86	1.80
29C	1.263	1.642	39.38	48.17	1.67	1.98
29D	1.242	1.682	39.00	48.94	2.32	1.98
29E	1.240	1.684	39.06	49.15	2.01	1.99
29F	1.185	1.683	41.24	51.96	1.97	1.94
30	1.219	1.641	39.53	49.12	2.43	2.06
31	1.067	1.599	51.14	56.15	1.86	1.85
32	1.156	1.670	45.30	51.90	1.78	1.79
33A	1.226	1.663	46.42	45.57	1.82	1.86
33B	1.214	1.675	39.87	47.24	1.75	1.82
34	1.518	1.966	24.42	40.02	2.12	1.73
35	1.622	1.938	19.50	32.21	2.24	2.26
36	1.648	1.984	20.38	35.23	1.54	2.08
37	1.616	1.959	21.27	36.28	1.91	1.75
38	1.671	2.003	23.90	35.16	1.26	2.23

4. Results and Considerations

4.1. Physical Properties of Hydrothermally Altered Rocks

The average of several physical properties of hydrothermally altered rocks were found to be in the following ranges: density ρ_d = 0.599–2.518 g/cm^3 (dry condition) and ρ_{sat} = 1.334–2.594 g/cm^3 (saturated condition); water absorption Q = 3.02–123.34%; effective porosity n = 7.55–74.91%; and elastic wave velocity V_p = 0.980–3.943 km/s (dry condition) and 1.076–4.280 km/s (saturated condition) (see Figure 6 and Table 3). As shown in Figure 7, strong correlations were found between density and water absorption, density and effective porosity, and water absorption and effective porosity. Among the hydrothermally altered rocks, the laumontite zone tuffaceous conglomerate (rock code 25) had the largest average density in the dry and saturated conditions, whereas the smectite zone fine tuff (rock code 18) had the smallest density. The smectite zone fine tuff (rock code 18) had the largest average water absorption and effective porosity of all the hydrothermally altered rocks, and the laumontite zone tuffaceous conglomerate (rock code 25) had the smallest values. The alunite-quartz zone dacite (rock code 2) had the largest average elastic wave velocity in the dry condition, while the laumontite zone lapilli tuff (rock code 24) had the smallest average elastic wave velocity. In the saturated condition, the laumontite zone tuffaceous conglomerate (rock code 25) had the largest average elastic wave velocity, and the halloysite zone tuffaceous conglomerate (rock code 6) had the smallest value.

4.2. PLS Index of Hydrothermally Altered Rocks

The average PLS indexes of hydrothermally altered rocks in the dry condition ranged from 0.12 to 3.52 MPa, while the average PLS indexes in the saturated condition ranged from 0.04 to 2.21 MPa (see Figure 6 and Table 2). The K-feldspar zone fine tuff in the dry condition had the largest average PLS index of all the hydrothermally altered rocks (rock code 10, 3.52 MPa), followed by the alunite-quartz zone weathered dacite (rock code 2, 3.06 MPa; Figure 6 and Table 2). The smectite zone pumice tuff in the dry condition had

the smallest value (rock code 20, 0.12 MPa), with smectite zone pumice tuff having the next lowest strength (rock code 21, 0.15 MPa; Figure 6 and Table 2). In the saturated condition, the alunite-quartz zone weathered dacite had the largest average PLS index (rock code 2, 2.21 MPa), followed by the laumontite zone tuffaceous conglomerate (rock code 25, 1.64 MPa; Figure 6 and Table 2). The smectite zone pumice tuff in the saturated condition had the smallest value (rock code 20, 0.04 MPa), with the halloysite zone tuffaceous conglomerate and the interstratified chlorite/smectite mineral zone fine tuff having the next lowest strength (rock code 6 and 15, respectively, 0.05 MPa; Figure 6 and Table 2). The average PLS indexes of hydrothermally altered rocks tended to be large for the alunite-quartz and K-feldspar zone rocks, and small for the halloysite, smectite, interstratified chlorite/smectite mineral, and interstratified illite/smectite mineral zone rocks, which are characterized by the presence of swelling clay minerals.

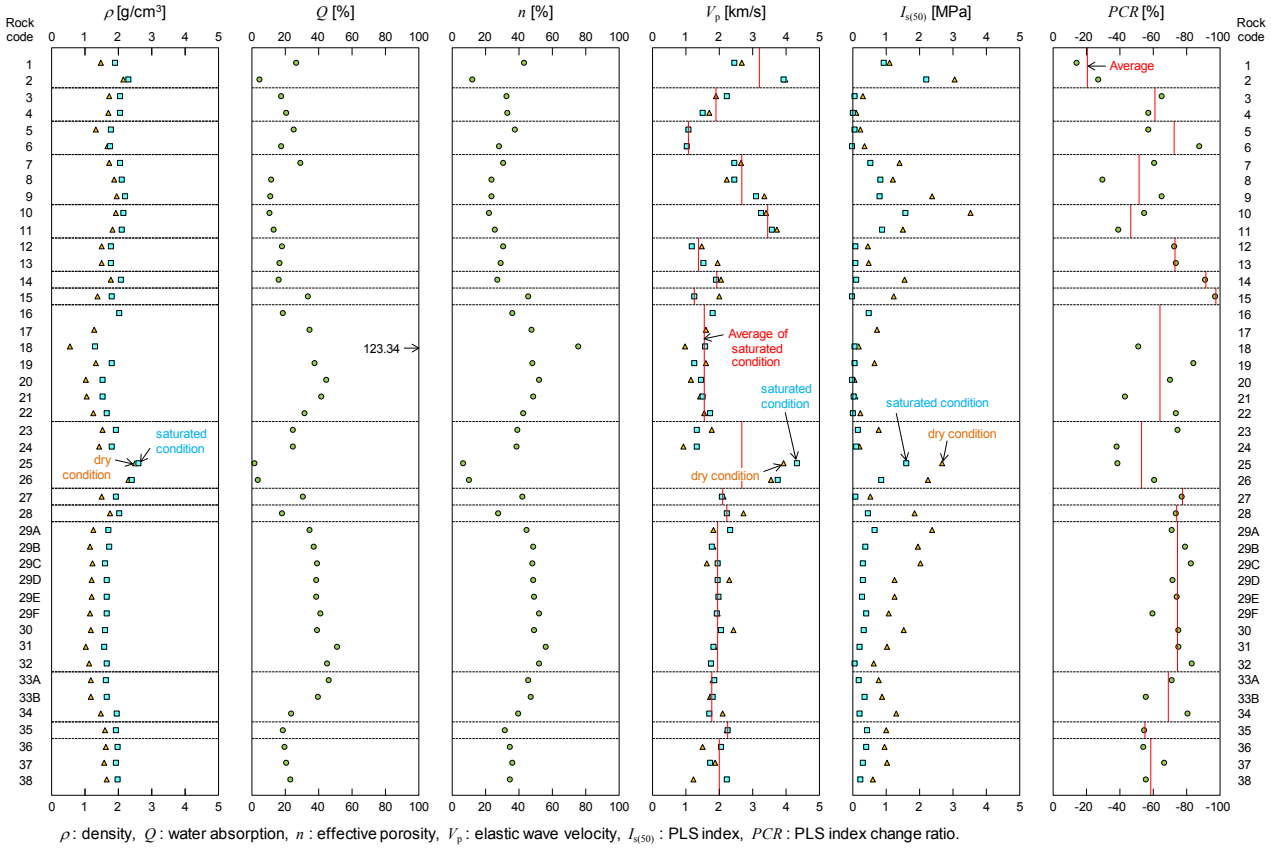

Figure 6. Physical and mechanical properties of hydrothermal altered rocks

We examined the PLS index decrease ratios for a range of rock. The strength change ratio can be represented by the formula

$$PCR = \frac{I_{s(50),dry} - I_{s(50),sat}}{I_{s(50),dry}} \times 100 \ (\%) \qquad (10)$$

where PCR is the PLS index change ratio, $I_{s(50),dry}$ is the PLS index of specimens in the dry condition, and $I_{s(50),sat}$ is the PLS index of specimens in the saturated condition. This equation expresses the difference in strength between dry and saturated conditions, where the strength value in the dry condition is 100 %. Figure 6 shows the PLS index change ratio of the rocks in hydrothermal alteration zones. The average PLS index change ratios of hydrothermally altered rocks ranged from 15.0 to 95.8%. The interstratified chlorite/smectite mineral zone fine tuff had the largest PLS index change ratio (rock code 15, 95.8%), followed by the interstratified illite/smectite mineral zone rocks (rock code 14, 89.9%; Figure 6 and Table 2). In contrast, the alunite-quartz zone dacite had the smallest value (rock code 1 and 2, 15.0 and 27.5%), with the propylitic zone medium tuff having the next lowest strength (rock code 8, 30.2%; Figure 6). The average of the PLS index change ratios exceeded 60% for the illite and zeolite zones, including the laumontite, analcite, heulandite, mordenite, clinoptilolite, and stilbite zones and for the halloysite, interstratified illite/smectite mineral, interstratified chlorite/smectite mineral, and smectite zones, which were characterized by the presence of swelling clay minerals. Maeda et al. [19] showed that the hydrothermal alteration products, smectite, mordenite, and laumontite were closely associated with ancient landslides. We noted that hydrothermal alteration zone landslides developed within very weak hydrothermally altered soft rocks such as those in the smectite, interstratified illite/smectite mineral, illite, mordenite, stilbite, heulandite, and laumontite zones. In addition, the occurrence of landslides in hydrothermal alteration zones was closely related to the presence of swelling clay

minerals and was independent of landslide size. Therefore, it is possible that surface and ground water cause a reduction in rock strength in these hydrothermal alteration zones, resulting in landslides. It was suggested that a PLS index change ratio of 60% will be used as the reference standard when predicting landslides. The results suggest that future landslide potential within a hydrothermal area can be assessed based on the hydrothermal alteration type and PLS index change ratio [3].

The discrepancies in the PLS test were calculated using a coefficient of variation

$$C_v = \frac{s}{I_{s(50),ave}} \times 100 \ (\%) \tag{11}$$

where C_v is the coefficient of variation, s is the standard deviation, and $I_{s(50),ave}$ is the average of the PLS test results. The coefficient of variation can be used to determine the number of specimens required for PLS testing. The number of specimens required to obtain results within ϕ = 25% of the average value over a one-sided interval at a 90% confidence level was 5, 7, and 10 for a C_v of 20, 30, and 40%, respectively. Figure 8 shows the correlation between the number of PLS test specimens and the coefficient of variation. A sufficient number of specimens were used for most of the PLS tests, except for three samples (Nos. 5, 6, and 29F of "rock code" in Table 2.). Therefore, the PLS testing methods established in this study were highly representative.

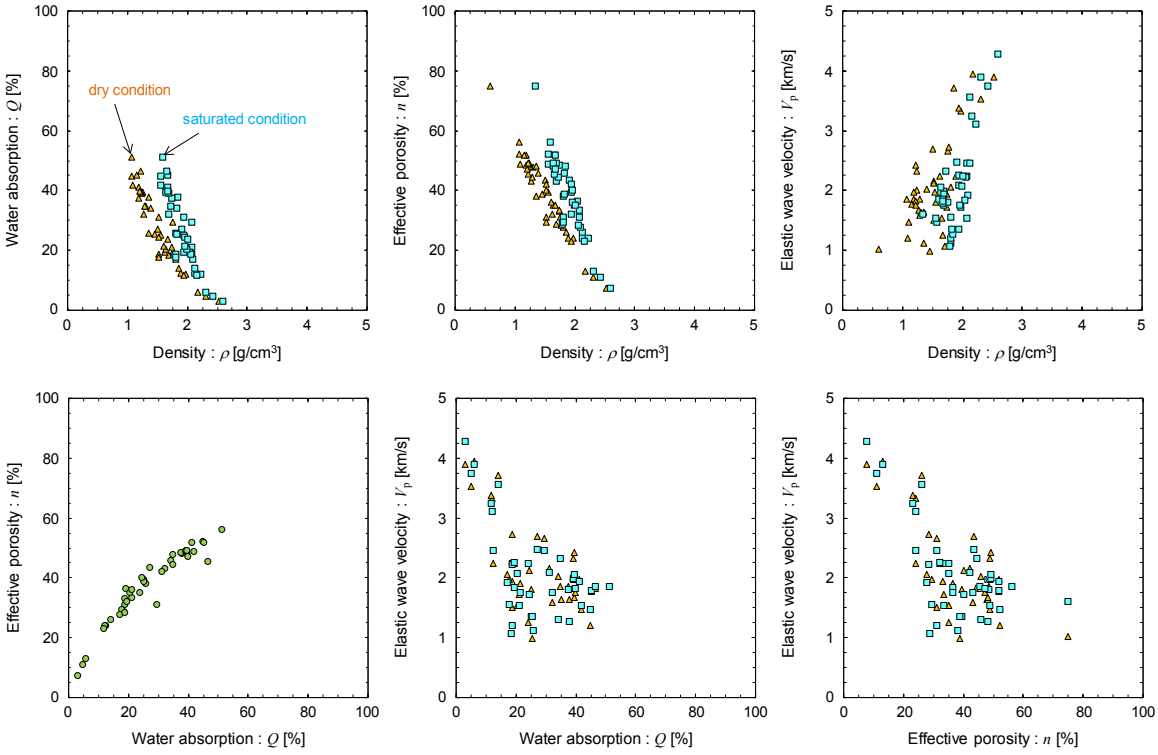

Figure 7. Correlations between the average value of physical properties of hydrothermal altered rocks

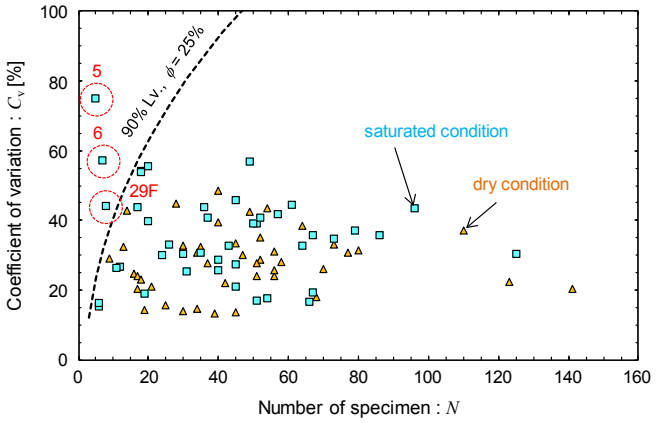

Figure 8. Correlation between number of specimen and coefficient of variation of the point load strength test. Numbers (5, 6, and 29F) of right graph correspond to ''Rock code'' in Tables 1 and 2

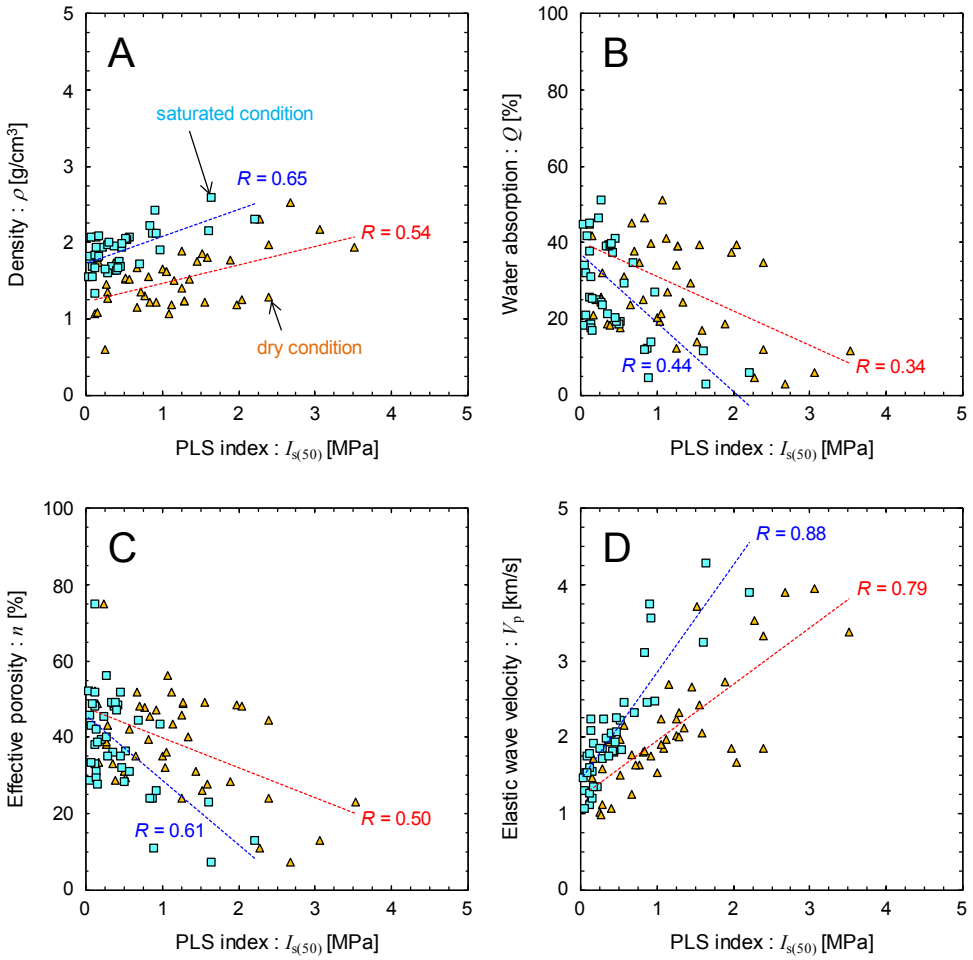

Figure 9. Correlations between point load strength index and physical properties. A: density, B: water absorption, C: effective porosity, D: elastic wave velocity

4.3. Correlation between PLS Index and Physical Properties of Hydrothermally Altered Rocks

Figure 9 shows the correlations between the PLS index and the physical properties of hydrothermally altered rocks. The PLS index increased with the density and elastic wave velocity and decreased with the water absorption and effective porosity. The PLS index and elastic wave velocity was strongly correlated with *R*-values of 0.79 (dry condition) and 0.88 (saturated condition), while no strong correlation was observed between the PLS index and other physical properties, for which the *R*-values ranged from 0.34 to 0.65. The average PLS index change ratio and average elastic wave velocity in the saturated condition are strongly correlated (Figure 10). These results suggest that the PLS index change ratio can be determined by measuring the elastic wave velocity.

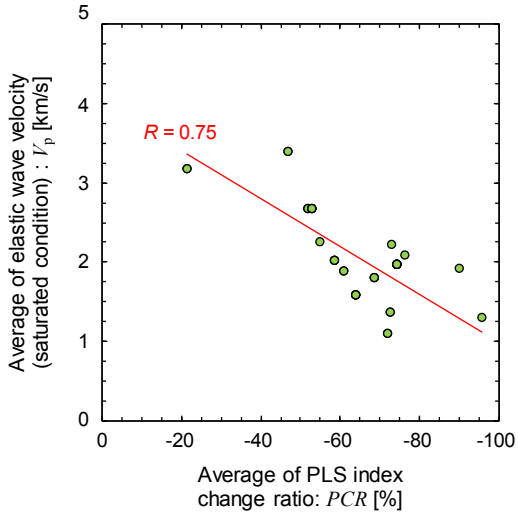

Figure 10. Correlations between average of point load strength index change ratio and average of elastic wave velocity under wet condition

5. Conclusions

The following is a summary of the correlations between the PLS index and physical properties of hydrothermally altered rocks.

Strong correlations were found between density and water absorption, density and effective porosity, and water absorption and effective porosity of the hydrothermally altered rocks. The PLS index increased with the density and elastic wave velocity and decreased with the water absorption and effective porosity. The PLS index was strongly correlated with the elastic wave velocity. The average PLS index change ratio and average elastic wave velocity in the saturated condition are strongly correlated. These results suggest that the PLS index change ratio can be determined by measuring the elastic wave velocity. The PLS index change ratio was closely associated with the ancient landslides. It was proposed that a PLS index change ratio of 60% could be used as reference standard when predicting landslides. The results suggest that future landslide and collapse potential within a hydrothermal area can be assessed based on the hydrothermal alteration type and PLS index change ratio.

Our data provide a basis for resource development, stability evaluation of underground utilization, landslide hazard assessment, and others.

REFERENCES

[1] G. Tsiambaos and N. Sabatakakis (2004): Considerations on strength of intact sedimentary rock. Engineering Geology, 72: 261–273.

[2] D. S. Agustawijaya (2007): The uniaxial compressive strength of soft rock. Civil engineering Dimension, 9: 9–14.

[3] M. Kohno and H. Maeda (2012): Relationship between point load strength index and uniaxial compressive strength of hydrothermally altered soft rocks, International Journal of Rock Mechanics and Mining Sciences, 50: 147–157.

[4] R. Ulusay, K. Türeli and M. H. Ider (1994): Prediction of engineering properties of a selected litharenite sandstone from its petrographic characteristics using correlation and multivariate statistical techniques, Engineering Geology, 38: 135–157.

[5] S. Kahraman (2001): Evaluation of simple methods for assessing the uniaxial compressive strength of rock, International Journal of Rock Mechanics and Mining Sciences, 38: 981–994.

[6] V. Palchik and Y. H. Hatzor (2004): The influence of porosity on tensile and compressive strength of porous chalks, Rock Mechanics and Rock Engineering, 37: 331–341.

[7] S. Kahraman, O. Gunaydin and M. Fener (2005): The effect of porosity on the relation between uniaxial compressive strength and point load index, International Journal of Rock Mechanics and Mining Sciences, 42: 584–589.

[8] İ. Çobanoğlu and S. B. Çelik (2008): Estimation of uniaxial compressive strength from point load strength, schmidt hardness and P-wave velocity, Bulletin of Engineering Geology and the Environment, 67: 491–498.

[9] A. Arel and A. Tugrul (2001): Weathering and its relation to geomechanical properties of Cavusbasi granitic rocks in northwestern Turkey, Bulletin of Engineering Geology and the Environment, 60: 123–133.

[10] A. Begonha and M. A. Sequeira Braga (2002): Weathering of the Oporto granite: geotechnical and physical properties, Catena, 49: 57–76.

[11] C. Chang, M. D. Zoback and A. Khaksar (2006): Empirical relations between rock strength and physical properties in sedimentary rocks, Journal of Petroleum Science and Engineering, 51: 223–237.

[12] N. K. Tamrakar, S. Yokota and S. D. Shrestha (2007): Relationships among mechanical, physical and petrographic properties of Siwalik sandstones, Central Nepal Sub-Himalayas, Engineering Geology, 90: 105–123.

[13] A. Binal (2009): Prediction of mechanical properties of non-welded and moderately welded ignimbrite using physical properties, ultrasonic pulse velocity, and point load index tests, Quarterly Journal of Engineering Geology and Hydrogeology, 42: 107–122.

[14] A. Pola, G. Crosta, N. Fusi, V. Barberini and G. Norini (2012): Influence of alteration on physical properties of volcanic rocks, Tectonophysics, 566-567: 67–86.

[15] A. Pola, G. B. Crosta, N. Fusi and R. Cactellanza (2014): General characterization of the mechanical behavior of different volcanic rocks with respect to alteration, Engineering Geology, 169: 1–13.

[16] H. Karakul and R. Ulusay (2013): Empirical Correlations for Predicting Strength Properties of Rocks from P-Wave Velocity Under Different Degrees of Saturation, Rock Mechanics and Rock Engineering, 46: 981–999.

[17] L. D. Wyering, M. C. Villeneuve, I. C. Wallis, P. A. Siratovich, B. M. Kennedy, D. M. Gravley and J. L. Cant (2014): Mechanical and physical properties of hydrothermally altered rocks, Taupo Volcanic Zone, New Zealand, Journal of Volcanology and Geothermal Research, 288: 76–93.

[18] L. D. Wyering, M. C. Villeneuve, I. C. Wallis, P. A. Siratovich, B. M. Kennedy and D. M. Gravley (2015): The development and application of the alteration strength index equation, Engineering Geology, 199: 48–61.

[19] H. Maeda, T. Sasaki, K. Furuta, K. Takashima, A. Umemura and M. Kohno (2012): Relationship between landslides, geological structures, and hydrothermal alteration zones in the Ohekisawa-Shikerebembetsugawa landslide area, Hokkaido, Japan, Journal of Earth Science and Engineering, 2: 317–327.

[20] M. Utada (1980): Hydrothermal alterations related to igneous activity in Cretaceous and Neogene formations of Japan. In: Granitic magmatism and related mineralization, S. Ishihara and S. Takenouchi (eds). Mining Geology, Special Issue, 67–83.

[21] ISRM Commission on Testing Methods, Working Group on Revision of the Point Load Test Method (1985): Suggested method for determining point load strength (Coordinator J. A.

Franklin). International Journal of Rock Mechanics and Mining Sciences and Geomechanics Abstract, 22: 51–60.

[22] ISRM Commission on Standardization of Laboratory and Field Tests (1979): Suggested method for determining water content, porosity, density, absorption and related properties and swelling and slake-durability index properties (Coordinator J. A. Franklin). International Journal of Rock Mechanics and Mining Sciences and Geomechanics Abstract, 16: 141–156.